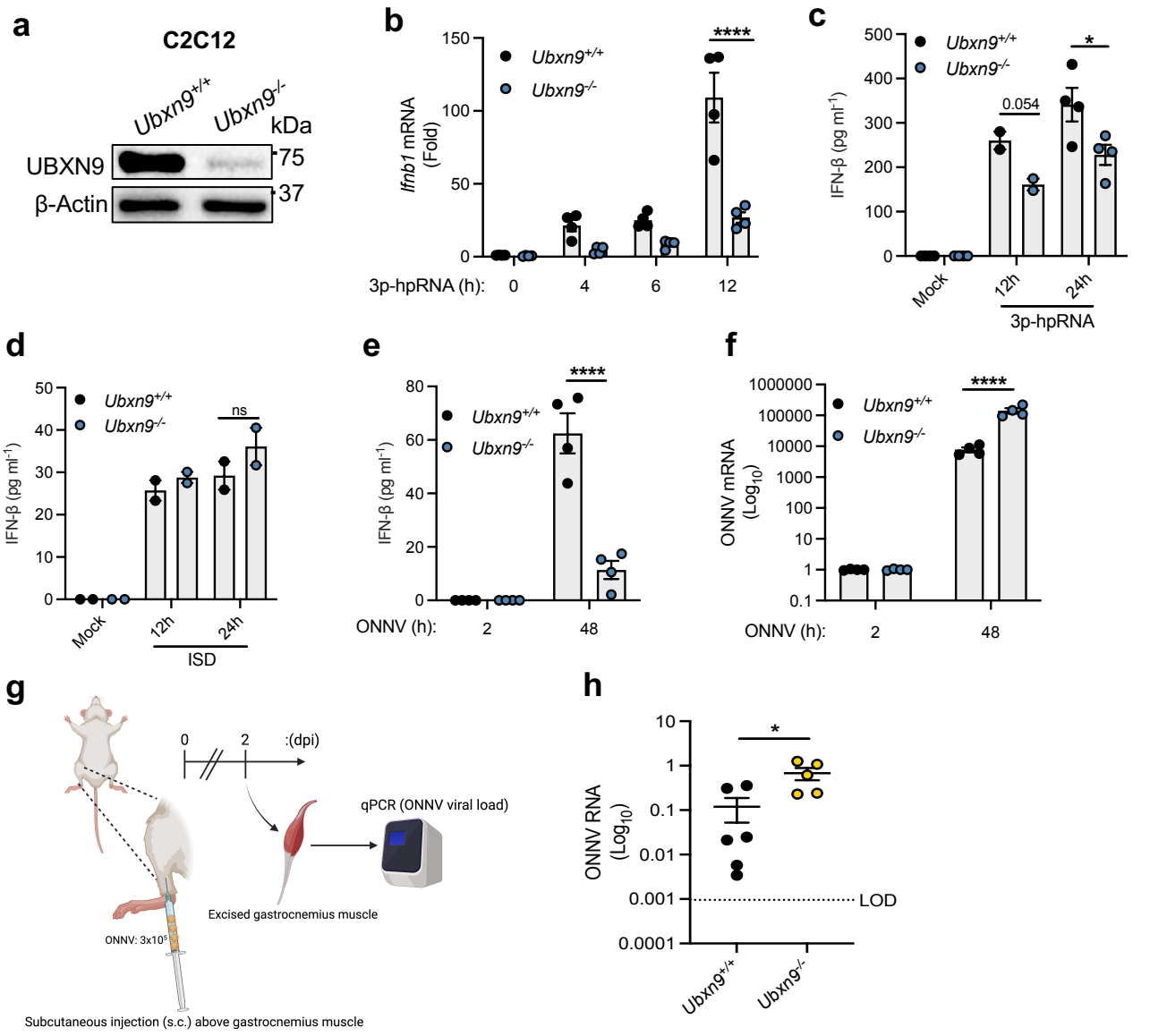

Supplemental Figure 1. UBXN9 is critical for RLR signaling *in vitro* and *in vivo*. Related to Figure 1. **a,** immunoblots of UBXN9 protein in *Ubxn9*$^{+/+}$ and *Ubxn9*$^{-/-}$ C2C12 myocytes. **b, c,** cellular *Ifnb1* mRNA levels (**b**) and secreted IFN-β protein concentrations (**c**) from C2C12 myocytes (n= 2-4 biological replicates) transfected with 3p-hpRNA. Mock, untreated. **d**, secreted IFN-β protein concentrations from C2C12 myocytes (n=2 biological replicates) transfected with interferon-stimulatory DNA (ISD). **e, f,** secreted IFN-β protein concentrations (**e**) and viral RNA loads (**f**) in mouse C2C12 cells (n=4 biological replicates) infected with ONNV (MOI: 1). **g, h,** age- and sex-matched *Ubxn9*$^{+/+}$ and *Ubxn9*$^{-/-}$ littermates (N=5-6 mice/group) infected with ONNV as depicted in (**g**), and viral RNA loads quantified by quantitative RT-PCR (**h**). Dpi: days post infection. The data are representative of 2-3 independent experiments (**b, c, e, f**) or 1 (**d**, **g,h**) independent experiment. Bar: mean ± SEM. *p<0.05, ****p<0.0001 by two-way ANOVA (**b-f**) or non-parametric Mann-Whitney test (**h**). LOD: limit of detection, established with uninfected mice (Mock).

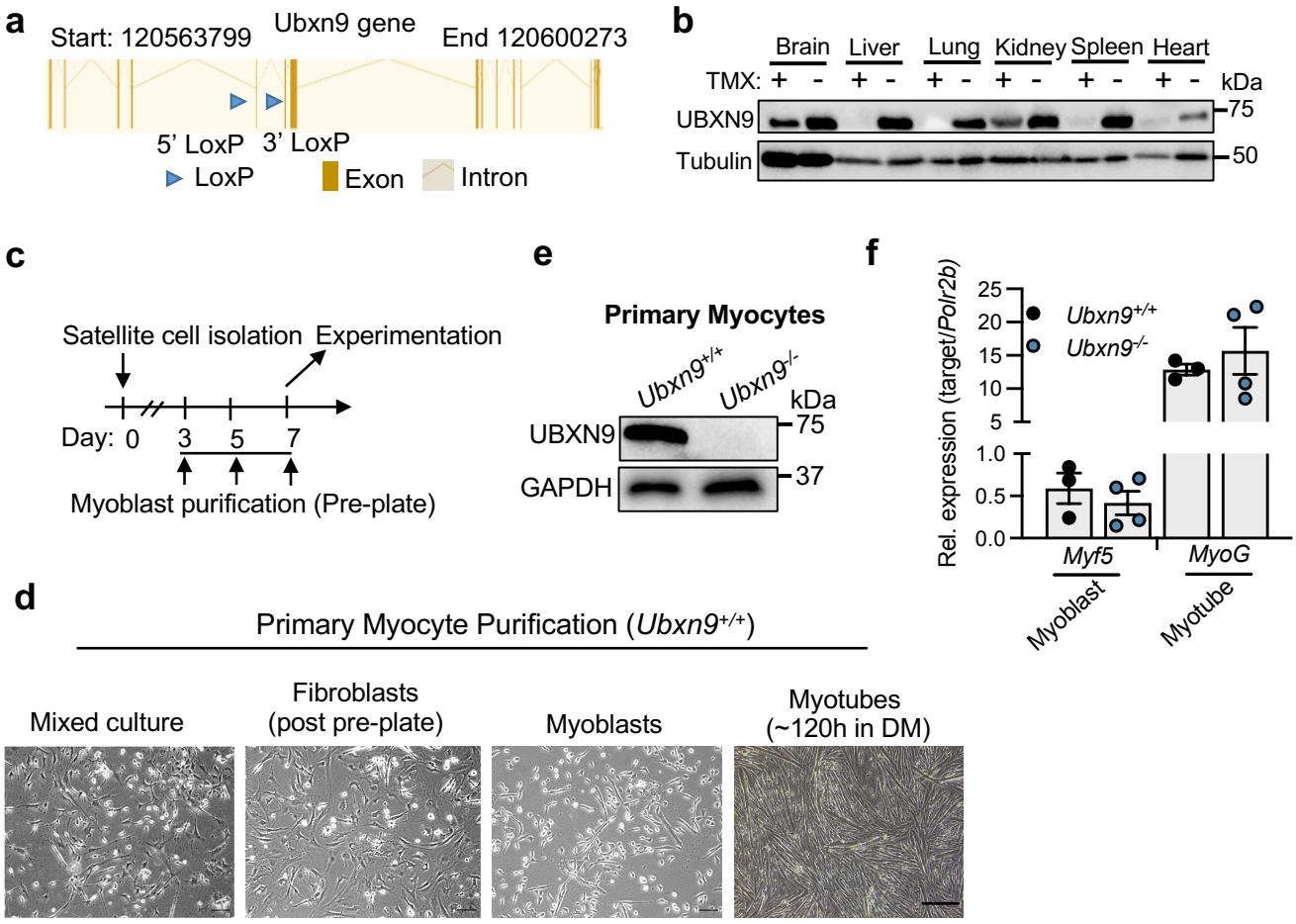

Supplemental Figure 2. The isolation and differentiation protocol of mouse primary myocytes. Related to Figure 1.

a, diagram illustrating the design of *Ubxn9*$^{flox/flox}$ mice where *loxP* sites flank Exon 5. Crossing of these mice with *Rosa26*$^{Cre-ERT2}$ and administration of tamoxifen (TMX) induces *Ubxn9* deletion (*Ubxn9*$^{-/-}$). **b**, immunoblots of UBXN9 and housekeeping Tubulin proteins in various tissues of *Ubxn9*$^{-/-}$ mice (+TMX) compared to *Ubxn9*$^{+/+}$ littermates (+ corn oil). **c,** protocol for isolation of mouse primary myoblast from *Ubxn9*$^{+/+}$ and *Ubxn9*$^{-/-}$ mice. **d,** representative light microscopic photos demonstrating pre-plating steps depicted in (**c**). Scale bar, 10μm. Cells were isolated from *Ubxn9*$^{+/+}$ mice as an example of the purification process. DM, differentiation medium. **e,** immunoblots of UBXN9 and GAPDH in purified myoblasts isolated from *Ubxn9*$^{+/+}$ and *Ubxn9*$^{-/-}$ mice. **f**, *Myf5* and *MyoG* mRNA expression in *Ubxn9*$^{+/+}$ and *Ubxn9*$^{-/-}$ myoblasts and myotubes, respectively. *Polr2b* serve as a housekeeping gene to quantify relative expression. Bar: mean ± SEM, n=3-4 mice/group from one experiment.

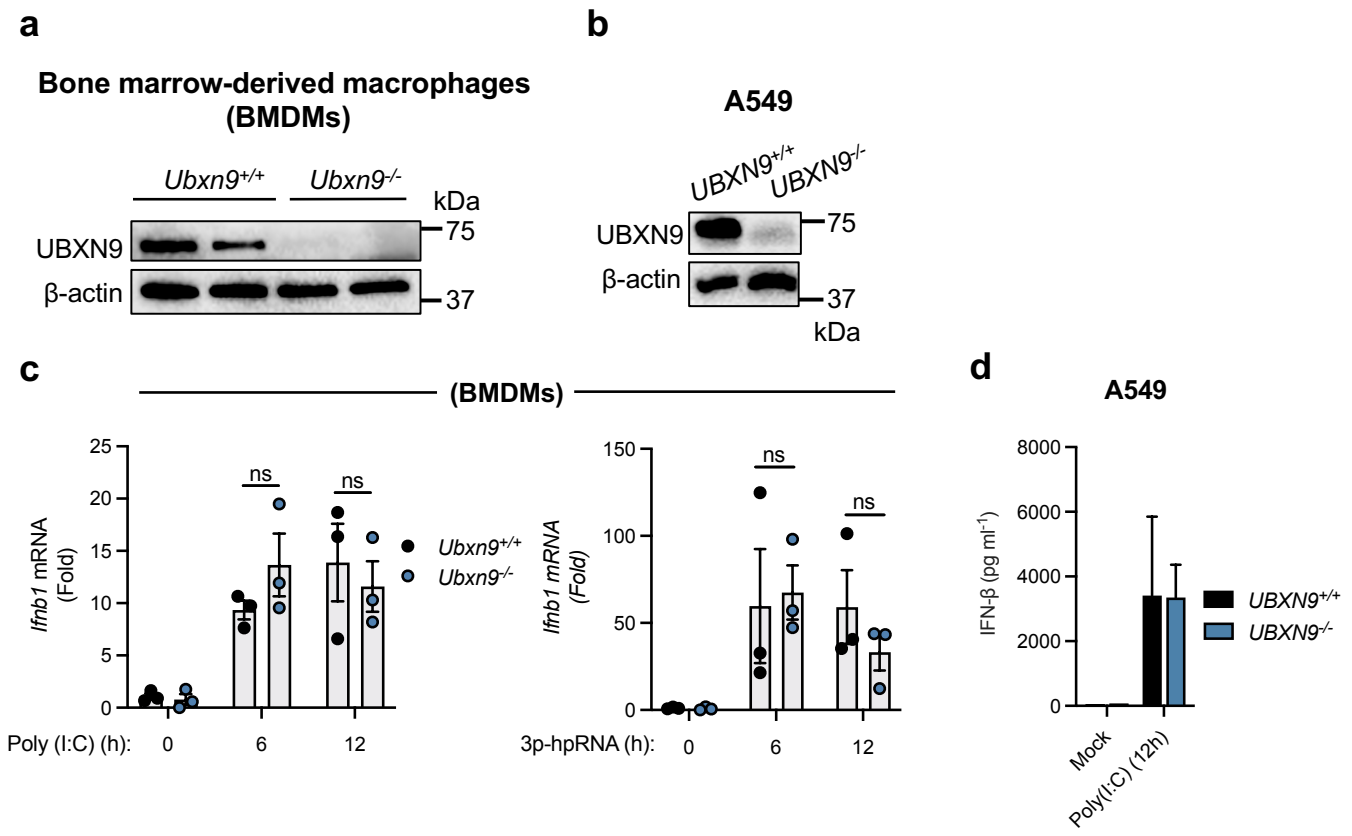

Supplemental Figure 3. UBXN9 does not influence RLR signaling in innate immune cells or the human lung A549 cell line. Related to Figure 1.
a, immunoblots of UBXN9 and β-actin in bone marrow-derived macrophages (BMDMs) isolated and differentiated from *Ubxn9*$^{+/+}$ and *Ubxn9*$^{-/-}$ mice (n=2 mice/group as a representative of UBXN9 knockout efficiency. **b,** immunoblots of UBXN9 and β-actin in *UBXN9*$^{+/+}$ and *UBXN9*$^{-/-}$ A549 lung cells. **c**, cellular *Ifnb1* transcript levels in *Ubxn9*$^{+/+}$ and *Ubxn9*$^{-/-}$ BMDMs (n=3 mice/group) before and after transfection with Poly(I:C) (left**)** or 3p-hpRNA (right). **d**, IFN-β protein concentrations from *UBXN9*$^{+/+}$ and *UBXN9*$^{-/-}$ A549 cells (n=2 biological replicates) stimulated with Poly(I:C) for 12h. The data are representative of 2 independent experiments. ns, not significant.

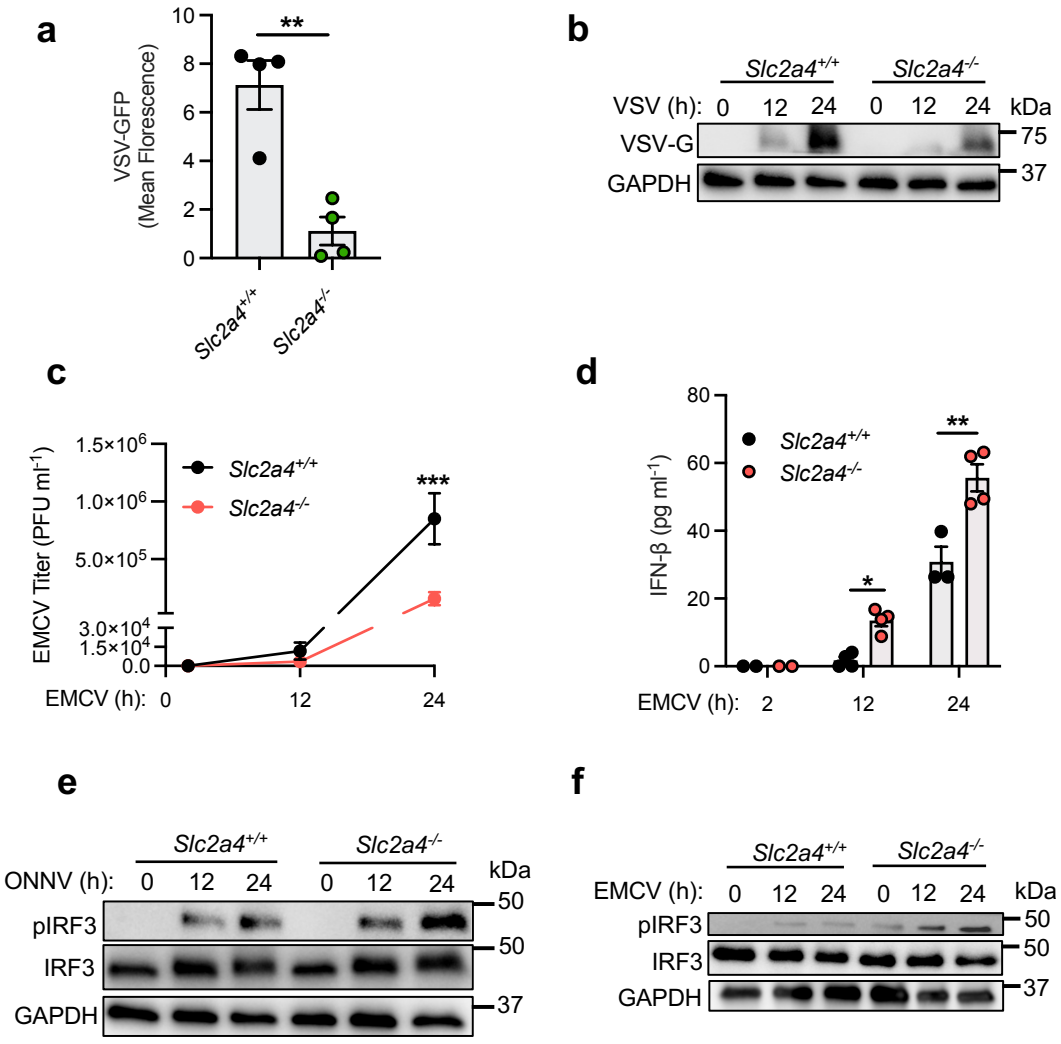

Supplemental Figure 4. GLUT4 inhibits RLR signaling in C2C12 myocytes. Related to Figure 2. **a,** mean fluorescence of VSV-GFP$^+$ in *Slc2a4*$^{+/+}$ and *Slc2a4*$^{-/-}$ C2C12 cells at 24 hours post-infection (hpi). VSV (MOI: 1). **b**, immunoblots of VSV-G protein in *Slc2a4*$^{+/+}$ and *Slc2a4*$^{-/-}$ C2C12 cells before and after VSV infection (MOI: 1). **c, d**, EMCV titers (**c**) and IFN-β protein levels (**d**) from *Slc2a4*$^{+/+}$ and *Slc2a4*$^{-/-}$ C2C12 cells (n=2-4 biological replicates) infected with EMCV (MOI: 0.5) PFU, plaque forming unit. **e, f,** immunoblots of phosphorylated (p) and total IRF3 before and after ONNV (**e**) or EMCV (**f**) infection in *Slc2a4*$^{+/+}$ and *Slc2a4*$^{-/-}$ C2C12 cells. EMCV MOI: 0.5; ONNV MOI: 1. The data are representative of 1 out of 2 independent reproducible experiments. Bar: mean ± SEM. *p<0.05, **p<0.01, ***p<0.001 by unpaired two-tailed Student's t-test (**a**) or two-way ANOVA (**c, d**).

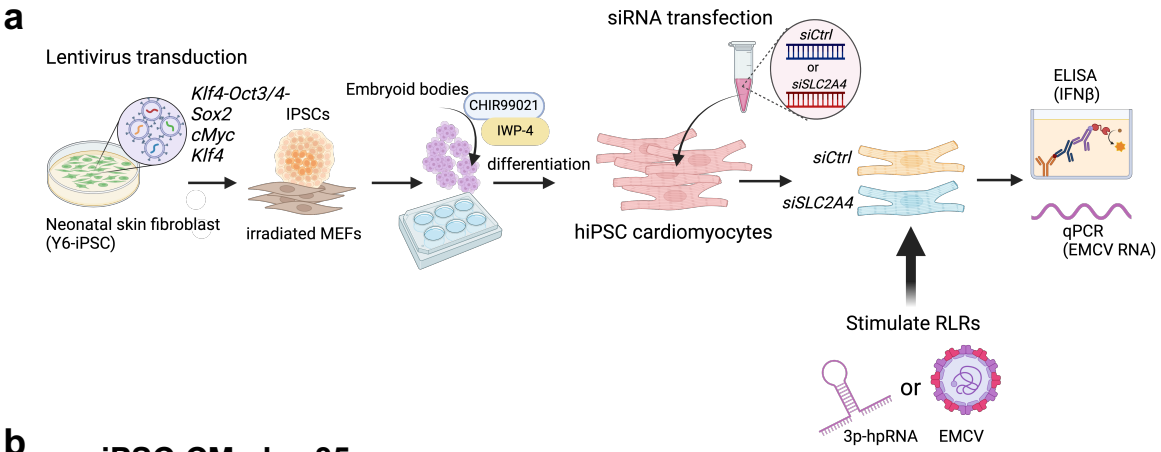

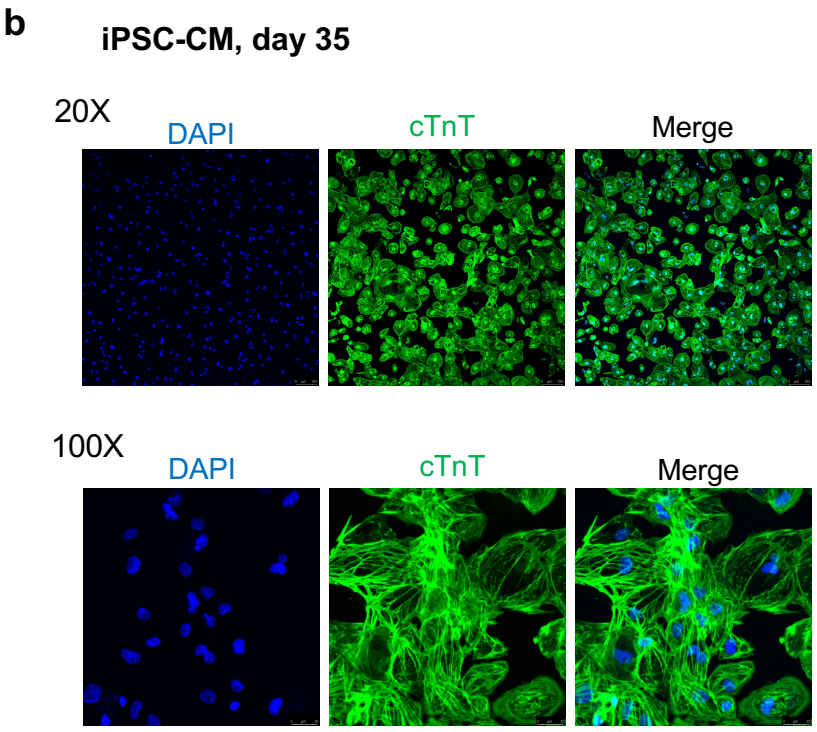

Supplemental Figure 5. Immunofluorescence confirmation of cardiac troponin T expression in induced pluripotent stem cell-derived cardiomyocytes (iPSC-CM). Related to Figure 2.
a, timeline and experimental protocol for the generation of induced pluripotent stem cells (iPSCs) and their differentiation into iPSC-derived cardiomyocytes (iPSC-CMs). iPSC-CMs were then transfected with control siRNA (*siCtrl*) or siRNA specific to GLUT4 (*siSLC2A4*) for 48h before assessing RLR responses. CHIR99021, GSK3 inhibitor/Wnt activator; IWP-4, inhibitor of Wnt production-4. **b**, confocal microscopic images of cardiac troponin T (cTnT) counterstained with DAPI (nuclear DNA) in iPSC-CM on day 35 of differentiation. Top panel, 20x magnification; bottom panel, 100x magnification. Scale bar, 100μm (top) and 25μm (bottom).

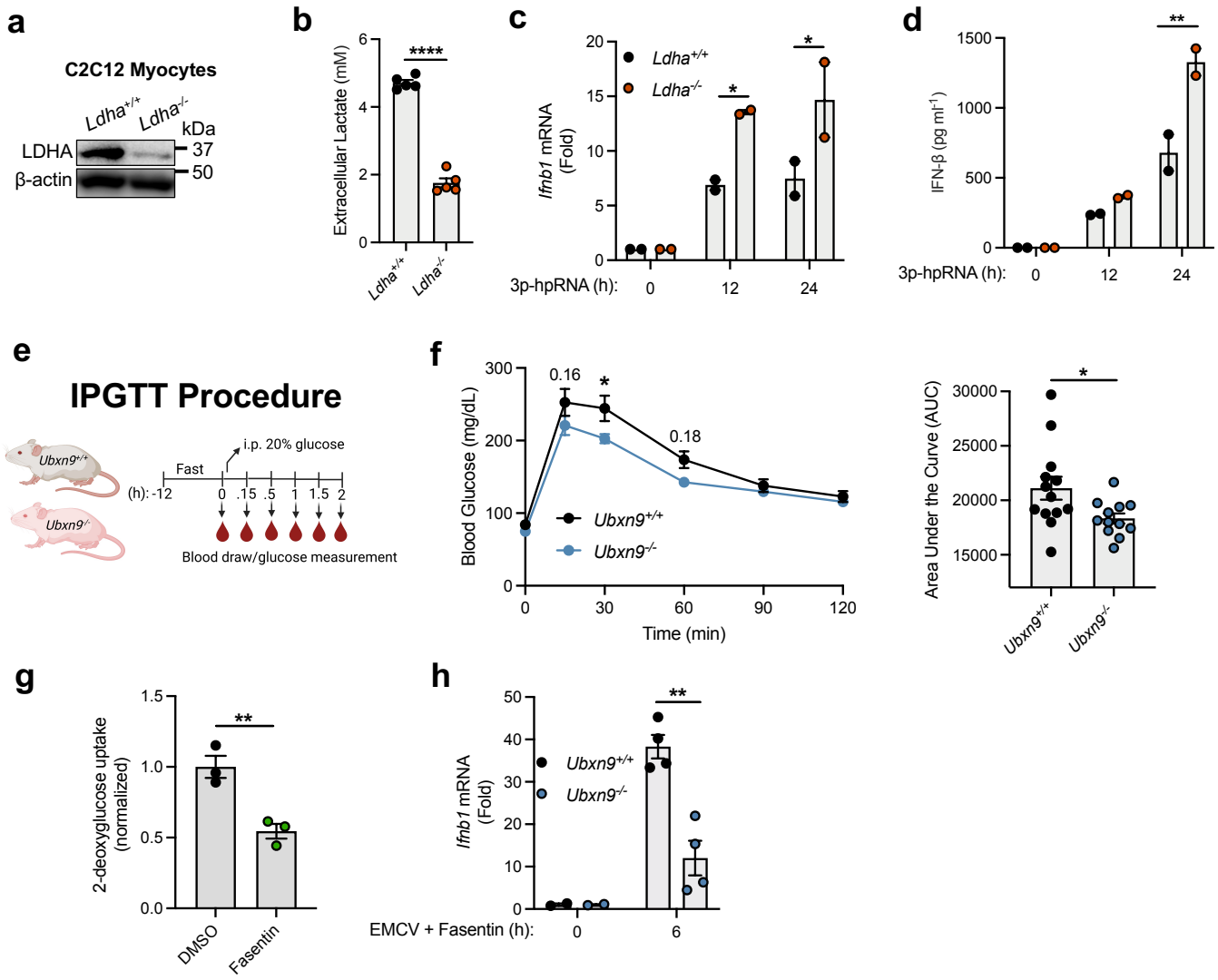

Supplemental Figure 6. RLR signaling is regulated by a lactate and glucose-independent mechanism despite increased glucose tolerance after Ubxn9 deletion Related to Figure 3.
a, b, immunoblots of LDHA and β-actin in *Ldha*$^{+/+}$ and *Ldha*$^{-/-}$ C2C12 myocytes (n= 5 biological replicates pooled from 2 independent experiments) (**a**) and extracellular lactate levels after 12 h of culture (**b**). The background lactate level in the cell culture medium (0 h) was subtracted. **c, d,** cellular *Ifnb1* transcripts in (**c**) and secreted IFN-β protein levels (**d**) from C2C12 cells (n=2 biological replicates) stimulated with 3p-hpRNA. **e**, age- and sex-matched *Ubxn9*$^{+/+}$ and *Ubxn9*$^{-/-}$ littermates underwent fasting for 12 h, then an intraperitoneal (i.p.) glucose tolerance test (IPGTT) with 1mg kg^{-1} of glucose. **f**, glycemia at the indicated times and area under curve (AUC) during the IPGTT. N=12-13/group pooled from 3 independent experiments. **g**, Glucose uptake in DMSO or Fasentin (25μM) pre-treated WT C2C12 cells. N=3 biological replicates/group. **h**, cellular *Ifnb1* transcripts in C2C12 cells simultaneously treated with Fasentin (25μM) and EMCV (MOI: 0.5) for 6h. N=4 biological replicates/group. Bar: mean ± SEM. *p<0.05, **p<0.01,****p<0.0001 by unpaired two-tailed Student's t-test (**b, f, g, h)** and two-way ANOVA (**c, d, f**).

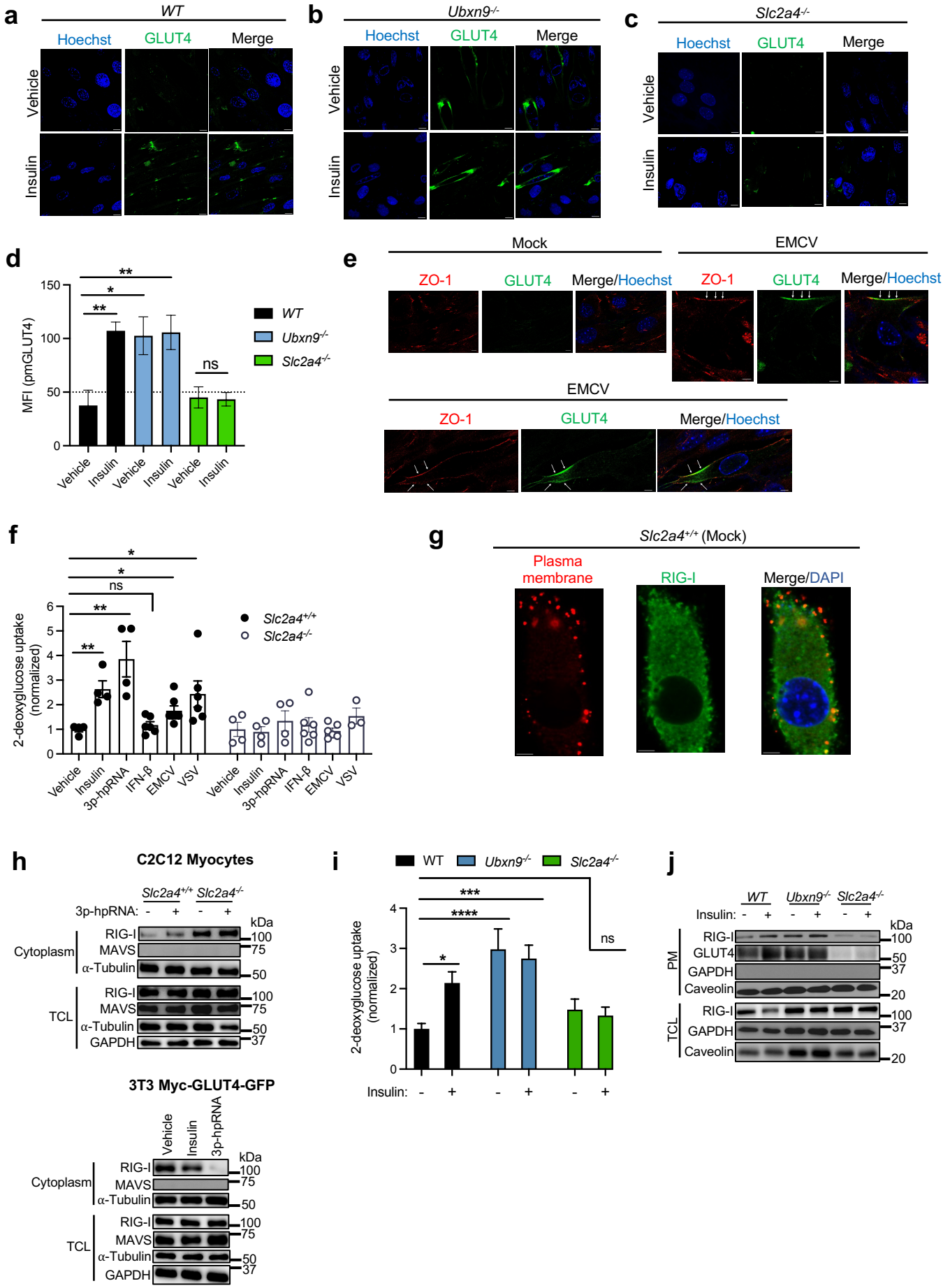
a
WT
Hoechst
GLUT4
Merge
Vehicle
Insulin
b
Ubxn9-/-
c
Slc2a4-/-
d
MFI (pmGLUT4)
150
100
50
0
**
*
ns
WT
Ubxn9-/-
Slc2a4-/-
Vehicle
Insulin
e
Mock
EMCV
ZO-1
GLUT4
Merge/Hoechst
f
2-deoxyglucose uptake (normalized)
ns
Slc2a4+/+
Slc2a4-/-
3p-hpRNA
IFN-β
EMCV
VSV
g
Slc2a4+/+ (Mock)
Plasma membrane
RIG-I
Merge/DAPI
h
C2C12 Myocytes
3p-hpRNA:
kDa
Cytoplasm
TCL
RIG-I
MAVS
α-Tubulin
GAPDH
3T3 Myc-GLUT4-GFP
i
WT
Ubxn9-/-
Slc2a4-/-
***
****
Insulin:
j
PM
GLUT4
Caveolin

Supplemental Figure 7. Insulin, 3p-hpRNA and virus infection promotes glucose uptake and RIG-I translocation to the plasma membrane in a GLUT4-dependent manner. Related to Figure 3 and 4. **a-c,** confocal images of endogenous GLUT4 (exofacial surface only) and nuclear DNA (Hoechst) in myocytes stimulated without (Mock) or with insulin (200 nM) for 20 min. Scale bar, 10 μm. **d**, mean fluorescence intensity (MFI) of plasma membrane GLUT4 (pmGLUT4) from cells (n= 7-11 individual images per treatment/group) stimulated as in (**a-c**). Dotted line indicates background fluorescence. **e**, confocal images of endogenous GLUT4 (exofacial surface only) and the plasma membrane marker ZO-1 in wild-type C2C12 myocytes before (Mock) or after EMCV infection (MOI: 0.5, 24h). Scale bar, 5 μm. Arrows indicate regions of GLUT4 and ZO-1 colocalizations after EMCV infection. **f**, 2-deoxyglucose (2-DG) uptake in *Slc2a4*$^{+/+}$ and *Slc2a4*$^{-/-}$ C2C12 cells treated with insulin (200 nM) for 20 min, transfected with hpRNA for 12 h, treated with IFN-β for 12 h, infected with EMCV (MOI: 0.5) for 24 h, or infected with VSV (MOI: 0.5) for 24h. The results are normalized to Mock of *Slc2a4*$^{+/+}$. **g**, confocal images of plasma membrane (PM) staining, RIG-I and nuclear DNA (DAPI) in C2C12 cells mock treated. Scale bar, 5 μm. **h,** cytoplasmic fraction from C2C12 myocytes (upper) and 3T3-L1 myc-GLUT4-GFP adipocytes (lower) subjected to subcellular fractionation before and after various treatments. α-Tubulin is housekeeping control for cytoplasmic fraction. Mock, transfection media alone; vehicle, DMSO alone. Insulin for 20min (200nM); 3p-hpRNA for 6h. **i**, glucose uptake by C2C12 cells (=9-12 biological replicates/group) treated with or without insulin for 20 min (200 nM). **j**, immunoblots of indicated proteins in the PM and TCL of C2C12 cells treated with or without insulin for 20 min (200 nM) as in (**i**). The data are representative of 2 independent reproducible experiments. Bar: mean ± SEM. For (**f**), N= 4-6 biological replicates/group, pooled from 2 independent experiments. *p<0.05, **p<0.01, ***p<0.001, ****p<0.0001 by one-way ANOVA (**d, f, i**).

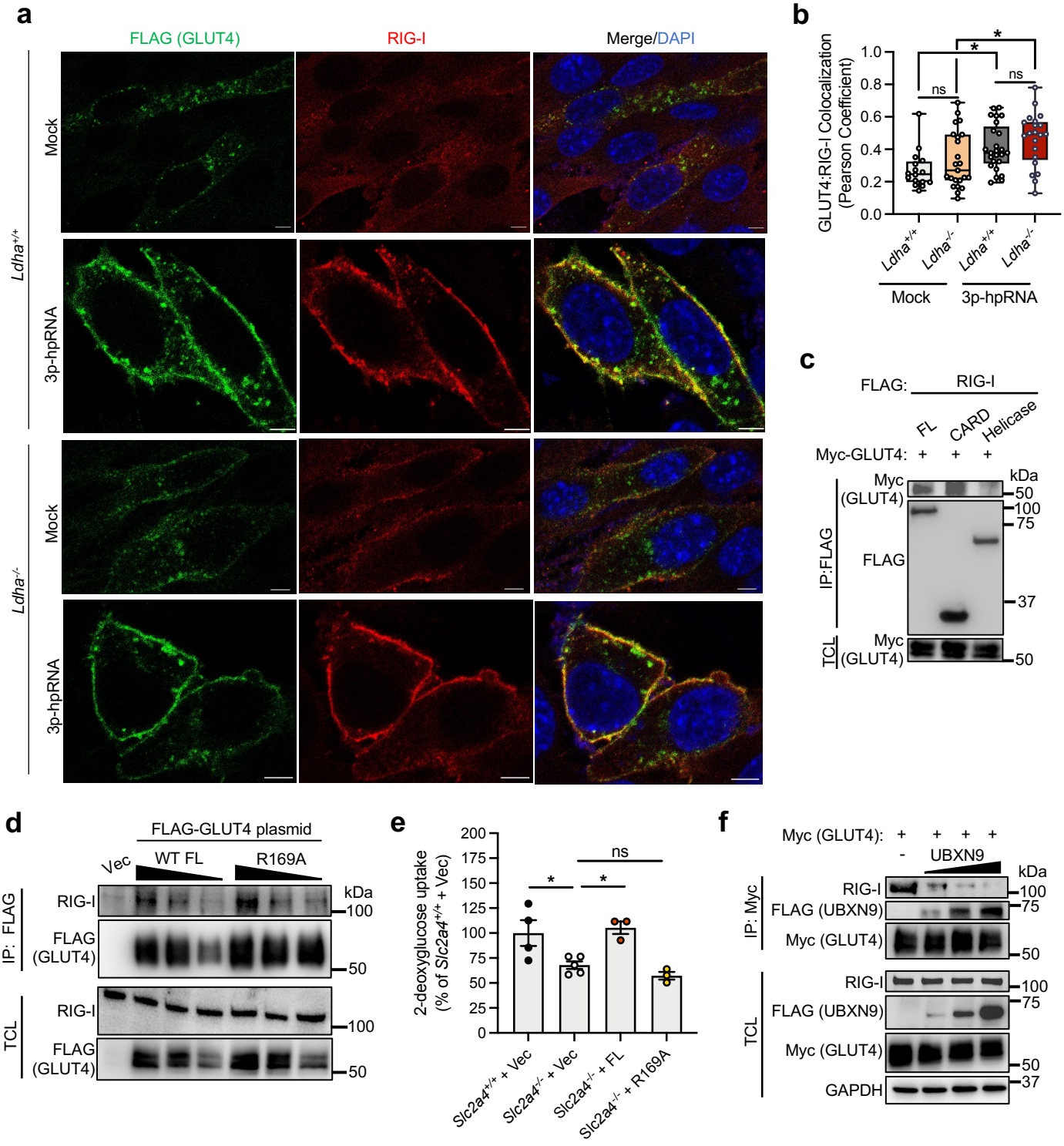

Supplemental Figure 8. **The CARD domain of RIG-I competes with GLUT4-UBXN9 binding in a glucose-uptake independent manner.** Related to Figure 5

a, confocal microscopic images of *Ldha*$^{+/+}$ and *Ldha*$^{-/-}$ C2C12 cells transfected with FLAG-GLUT4 for 24h before 3p-hpRNA treatment for 12h. Scale bar, 10 μm. Mock, transfection reagent only. **b**, GLUT4-RIG-I colocalization (N=16-25 fields/group) before and after 3p-hpRNA treatment from cells in (**a**). **c**, co-IP of the WT, CARD domain and helicase domain of RIG-I (FLAG) with GLUT4 (Myc) in HEK293T cells. Experiment is a repeat of **Fig. 5i** to equalize the FLAG protein for FL and the helicase domain of RIG-I for IP. **d**, co-IP of various doses of FLAG-WT (FL) or R169A GLUT4 with endogenous RIG-I from HEK293T cells. **e**, 2-deoxyglucose uptake levels in *Slc2a4*$^{-/-}$ cells reconstituted with GLUT4 plasmids as in (**d**). Cells were transfected with either vector (Vec), FLAG-FL or FLAG-R169A and then treated with insulin for 20 min (200nM). *Slc2a4*$^{+/+}$ cells transfected with Vec served as the positive control. **f**, co-IP of GLUT4 (Myc) with endogenous RIG-I in the presence of increasing concentrations of UBXN9 (FLAG) plasmid in HEK293T cells. The results are representative of 2 independent experiments. Bar: mean ± SEM. *p<0.05 by one-way ANOVA (**b**) or unpaired two-tailed Student's t-test (**e**).

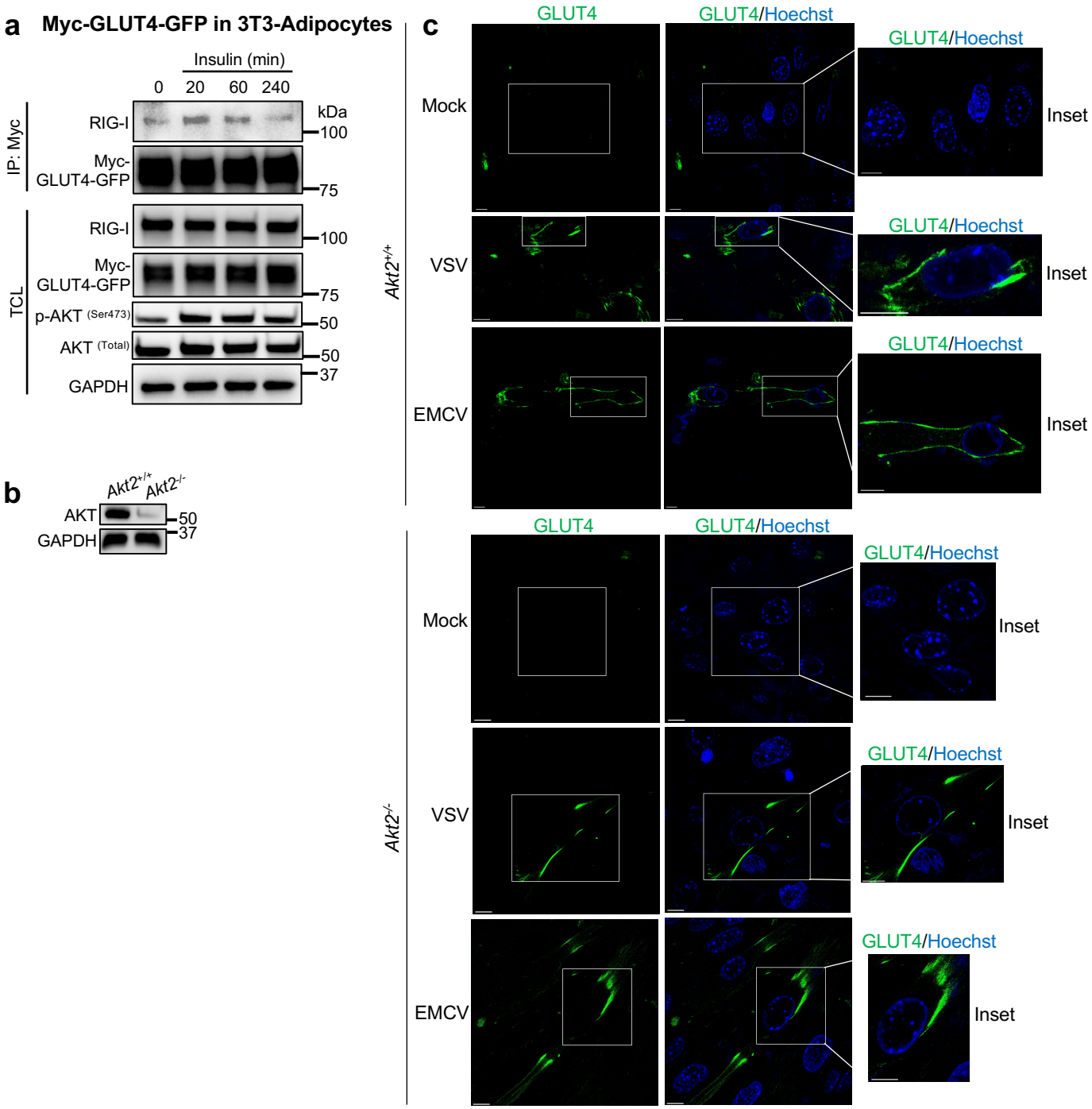

Supplemental Figure 9. AKT2 is dispensable for GLUT4 translocation in C2C12 myocytes. Related to Figure 5 and 6.

a, co-IP from 3T3-L1 myc-GLUT4-GFP adipocytes either mock treated or stimulated with insulin (200nM) for 20-, 60- or 240-min. **b**, immunoblot of AKT2 in *Akt2*$^{+/+}$ and *Akt2*$^{-/-}$ C2C12 cells. **c**, confocal microscopic images of exofacial GLUT4 and nuclear DNA (Hoechst) in *Akt2*$^{+/+}$ and *Akt2*$^{-/-}$ myocytes before and after VSV (MOI: 0.5) or EMCV (MOI: 0.5) infection for 12h. Scale bar, 10 μm. Mock, medium alone without virus. Results are representative of 2 independent experiments.

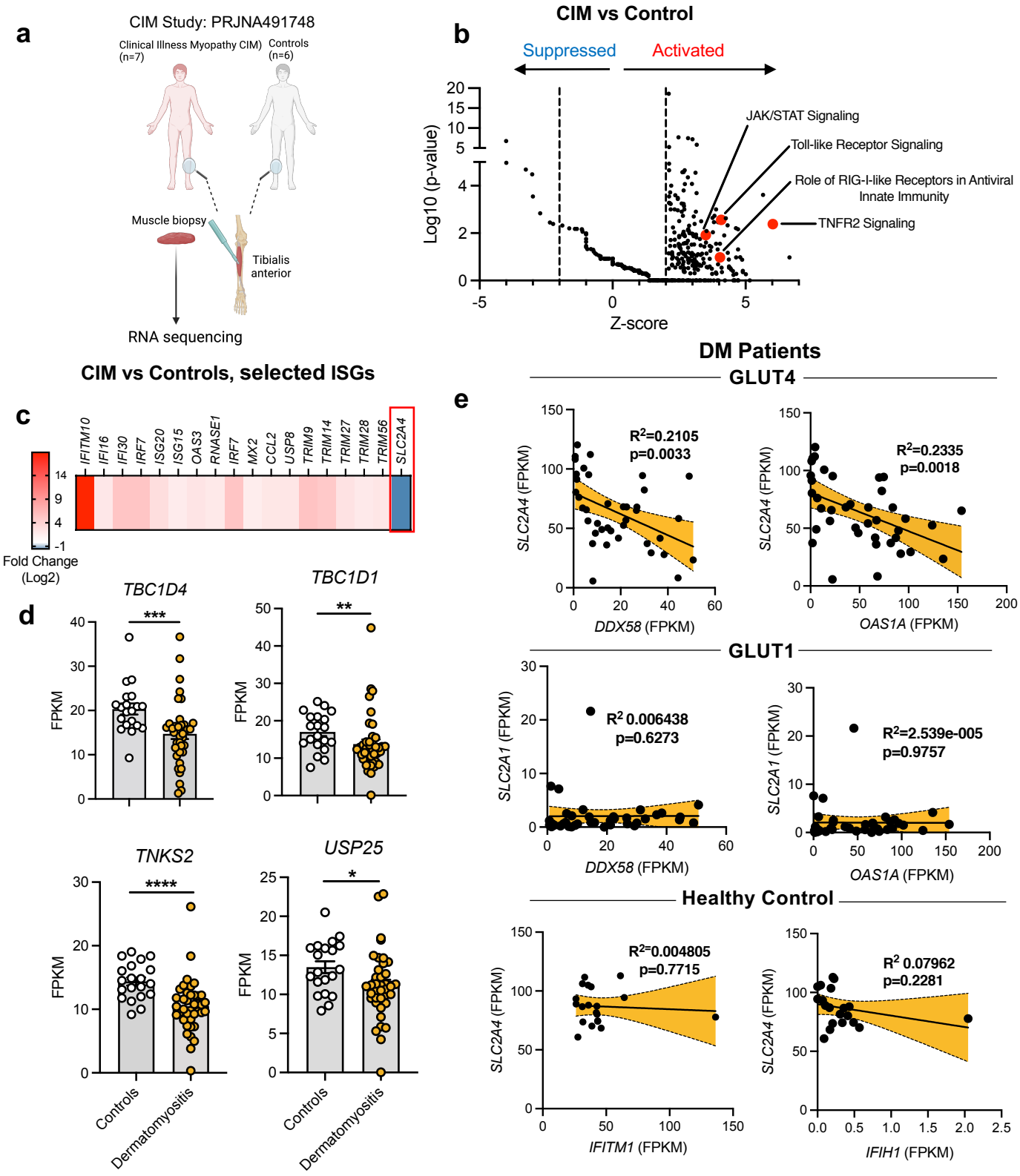

Supplemental Figure 10. Myopathic diseases are associated with decreased expression of GLUT4 and its trafficking machinery. Related to Figure 7.

a, schematic overview of critical illness myopathy (CIM) study. N=7 CIM and 6 healthy controls. **b**, Ingenuity Pathway Analysis (IPA) of the 6,257 differentially expressed genes (DEGs) ($p<0.05$, fold change ≥ 1.5) in the CIM patients compared to healthy controls. Red circles highlight innate-immune pathways activated in CIM patients compared to controls. **c**, select DEGs in the canonical interferon pathways and *SLC2A4* (GLUT4, red box) from (**b**). **d**, FPKMs of GLUT4 trafficking-related genes in dermatomyositis (DM) patients and healthy controls. **e**, simple linear regression analysis of *SLC2A4* or *SLC2A1* FPKMs with *DDX58* and *OAS1A* FPKMs in DM patients and healthy controls (*IFITM1*, *IFIH1*). Bar: mean ± SEM. **p*<0.05, ***p*<0.01, ****p*<0.0001, *****p*<0.00001 by Mann-Whitney test (**d**).